Consistency Conditions in MRI-based Attenuation Correction for Hybrid PET/MRI scanners

Zhengyi Yang[1], Viktor Vegh[1], Ian Turner[2], and David Reutens[1]

[1]*Center for Advanced imaging, The University of Queensland, Brisbane, Queensland, Australia,* [2]*School of Mathematical Sciences, Queensland University of Technology, Brisbane, Queensland, Australia*

Introduction: Combined PET/MRI scanners are currently the focus of extensive research and development (1, 2). This new generation of medical imaging devices combines the capabilities of positron emission tomography (PET) to obtain metabolic information with high sensitivity, and of magnetic resonance imaging (MRI) for structural and functional imaging without the additional radiation exposure associated with X-ray computerised tomography (CT). A major hurdle in the development of PET/MRI is correction for photon attenuation (3), which has a large effect on the accuracy of PET imaging. Inadequate attenuation correction has serious implications, for example, leading to inaccurate cancer staging or failure to detect tumours (4).

Attenuation correction relies on the calculation of an attenuation map representing the tissue-specific photon attenuation coefficient of each voxel. Attenuation correction with CT or with transmission PET scans suffers from the drawbacks of exposure to ionizing radiation and additional scan time both of which are circumvented if attenuation effects can be corrected accurately using data from MR scans acquired simultaneously with PET. This task is much more challenging than with CT because the attenuation coefficient and MR signal intensity are not directly linked as is the case with CT. PET emission data, organized as sinogram, contains information that can aid the construction of an attenuation map. This information is described as Helgason-Ludwig consistency conditions (HLCC) that put constraints on the moments of a radon transform (5-7). In this study, the efficacy of HLCC in finding appropriate attenuation coefficients of each voxel was verified on a simulated dataset.

Methods: These are a set of mathematical rules derived from the 2D Radon transform. PET sinogram data are projections of the radiotracer concentration and because the moments of projections through an object are periodic in azimuthal angle, HLCC exist and can be understood in terms of the following formulation:

$$\Phi_{m,k} = \int_0^{2\pi} \int_{-\infty}^{+\infty} s^m e^{ik\phi} e^{A(s,\phi)} E(s,\phi) ds d\phi$$

where $E(s,f)$ denotes measured data, $A(s,f)$ the projections of the attenuation coefficient map, m the moment being computed, and *k* the Fourier component. The radial distance from the centre of rotation s and the azimuthal angle of rotation f index Radon transform space. Attenuation corrected projection data should obey the consistency conditions that $\Phi_{m,k} = 0$ when $k > m$ or when $k + m$ is odd. Inaccurate attenuation correction should result in the violation of the conditions and non-zero coefficients in the Fourier transform of the moments of the emission data.

An insight from earlier studies is that use of a constant attenuation coefficient across subjects for each tissue class may introduce errors. For example, Salomon et al. (8) found that the attenuation coefficient of lung could vary by 10% across patients and described a method for estimating the attenuation coefficient from emission data by minimising inconsistency. In reality, some deviations from the HLCC may occur because of the discontinuity of data sampling in PET imaging (9) and because emission and detection of radiation do not occur within a zero-width projection line of response. In this work, we used brain [18F] fluorodeoxyglucose (FDG) PET/CT and MRI data acquired from the same patient. The ground truth attenuation map was derived from the CT image using multi-level Otsu threshold segmentation to create

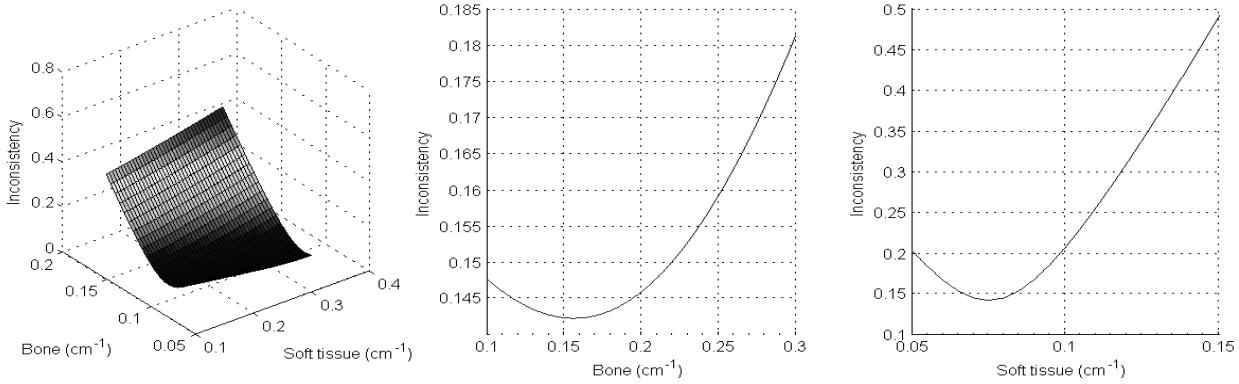

(a) Sinogram inconsistency and attenuation coefficients

(b) Cross section for soft tissue coefficient fixed at 0.075 cm^{-1}

(c) Cross section for bone coefficient fixed at 0.155 cm^{-1}

Figure 1. Inconsistency of attenuation corrected sinogram using combinations of attenuation coefficients for soft tissue and bone. Cross sections show that there is a global minimum.

a three class (air, soft tissue and bone) classification. Inconsistency of the sinogram was calculated for various combinations of attenuation measures for bone and soft tissue, with the coefficient for air fixed at 0. The measure of inconsistency was the sum of the Fourier coefficients

$\Phi = \sum_{m=0}^{k} \sum_{k=\{C_m\}} \Phi_{m,k}$, where C_m varies for each moment and the entries satisfy $m < k \leq 9$ or ($k \leq 9$ and $k + m$ is odd). The effect of a lesion with high uptake such as a metabolically active tumour was simulated on single slice by embedding in the deep white matter a 120 mm^2 region containing voxels with values above the 95th percentile of intensity. The sinogram was simulated by forward projection.

Results & Discussion:

As shown in Figure 1, for the normal brain, inconsistency was minimized for a combination of coefficients of 0.155 cm^{-1} for bone and 0.075 cm^{-1} for soft tissue compared to the ground truth values of 0.15 cm^{-1} for bone 0.095 cm^{-1} for soft tissue. For the brain with lesion, consistency was maximised for attenuation coefficients of 0.155 cm^{-1} for bone and 0.075 cm^{-1} for soft tissue implying that the lesion did not affect the inconsistency measure significantly. These results indicate that by maximizing the consistency of the sinogram accurate attenuation coefficient can be found for each tissue class and consistency conditions are robust to brain lesions.

References:

1. Herzog H, et al. NeuroImage. 2010;49(3):2072-82.
2. Pichler B, et al. European Radiology. 2008;18(6):1077-86.
3. Zaidi H, et al. PET Clinics. 2007;2(2):191-217.
4. Huang SC, et al. Journal of computer assisted tomography. 1979;3(6):804.
5. Bronnikov AV. IEEE TMI. 2000;19(5):451-62.
6. Bromiley A, et al. IEEE TNS. 2001;48(4):1371-7.
7. Alessio AM, et al. Medical Physics. 2010;37:1191.
8. Salomon A, et al. IEEE TMI. 2011;30(3):804-13.
9. Herraiz JL, et al. IEEE 2007 NSS'07.